Atomic Data and Nuclear Data Tables 151 (2023) 101573

Contents lists available at ScienceDirect

Atomic Data and Nuclear Data Tables

journal homepage: www.elsevier.com/locate/adt

Complete collision data set for electrons scattering on molecular hydrogen and its isotopologues: IV. Vibrationally-resolved ionization of the ground and excited electronic states

Liam H. Scarlett [a,b,*], Eric Jong [b], Starsha Odelia [b], Mark C. Zammit [c], Yuri Ralchenko [d], Barry I. Schneider [d], Igor Bray [b], Dmitry V. Fursa [b]

[a] Max–Planck-Institut für Plasmaphysik, Garching 85748, Germany
[b] Curtin Institute for Computation and Department of Physics and Astronomy, Curtin University, Perth, Western Australia 6102, Australia
[c] Theoretical Division, Los Alamos National Laboratory, Los Alamos, NM 87545, USA
[d] National Institute of Standards and Technology, Gaithersburg, MD 20899-8422, USA

ARTICLE INFO

Article history:
Received 26 October 2022
Received in revised form 9 January 2023
Accepted 9 January 2023
Available online 31 January 2023

Dataset link: https://mccc-db.org

ABSTRACT

We present a comprehensive set of vibrationally-resolved cross sections for electron-impact ionization of molecular hydrogen and its isotopologues (H_2, D_2, T_2, HD, HT, and DT) in both the ground and excited electronic states. We apply the adiabatic-nuclei molecular convergent close-coupling (MCCC) method to calculate cross sections from threshold to 1000 eV for ionization of the ground and excited vibrational levels of the $X\,^1\Sigma_g^+$, $B\,^1\Sigma_u^+$, $C\,^1\Pi_u$, $EF\,^1\Sigma_g^+$, $a\,^3\Sigma_g^+$, and $c\,^3\Pi_u$ electronic states, representing all states with united-atoms-limit principle quantum number $n=1$–2. The cross sections are presented in graphical form and provided as both numerical values and analytic fit functions in supplementary data files. The data can also be downloaded from the MCCC database at mccc-db.org.

* Corresponding author at: Curtin Institute for Computation and Department of Physics and Astronomy, Curtin University, Perth, Western Australia 6102, Australia.
E-mail address: liam.scarlett@protonmail.com (L.H. Scarlett).

https://doi.org/10.1016/j.adt.2023.101573
0092-640X/

Contents

1. Introduction

Electron collisions with molecular hydrogen and its isotopologues are processes of fundamental importance for the modeling of astrophysical, technological, and fusion plasmas. Ionization of these species is of particular interest in non-equilibrium plasmas, such as those used in semiconductor fabrication or present in the edge and divertor regions of tokamak fusion reactors [1]. With the present series of papers we aim to produce a complete set of vibrationally-resolved cross sections for electron scattering on H_2, D_2, T_2, HD, HT, and DT, calculated using the adiabatic-nuclei (AN) molecular convergent close-coupling (MCCC) method, with a particular focus on generating the necessary input data for collision-radiative (CR) models [2]. One of the distinctive features of the data is that it is self consistent, since the cross sections for all processes are extracted from a single set of scattering calculations which utilize a well-established unitary theory with an *ab initio* treatment of the coupling between all electronic reaction channels [3].

The previous installments in this series [4–6] presented a complete set of fully vibrationally-resolved cross sections for excitation of the $n = 2$–3 states from the $X\,^1\Sigma_g^+$ state of H_2 and its isotopologues, as well as cross sections for the excitation-radiative-decay process. Now, we turn our attention to electron-impact ionization of H_2 and its isotopologues, considering scattering on the ground state and both electronically- and vibrationally-excited states.

Ionization of H_2 and D_2 in the $X\,^1\Sigma_g^+(v_i = 0)$ state has been previously studied extensively. Numerous measurements have been reported, and Yoon et al. [7,8] have compiled recommended values for the ionization cross section based on the available data. Theoretical studies of the $H_2(X\,^1\Sigma_g^+, v_i = 0)$ ionization cross section have been performed using the *R*-matrix with pseudostates (RMPS) method [9] and the time-dependent close-coupling method [10], while Liu and Shemansky [11] have provided estimates for ionization of all bound vibrational levels of the $H_2(X\,^1\Sigma_g^+)$ state using a modified Born method. Celiberto et al. [12] utilized the semiclassical Gryzinski theory along with the Franck–Condon approximation to calculate cross sections for ionization of all bound vibrational levels of the $X\,^1\Sigma_g^+$ state of H_2 and D_2, and Wünderlich [13] applied the same method to vibrationally-resolved ionization of the first six non-dissociative electronic states of H_2. There is good agreement between the various theoretical and experimental results for ionization of the $X\,^1\Sigma_g^+(v_i = 0)$ state of H_2, but data for the isotopologues or for scattering on excited electronic or vibrational levels is too scarce to draw any conclusions [8]. The theoretical results of Wünderlich [13] are the most comprehensive data presented until now, and are in good agreement with experiment and *ab initio* quantum-mechanical calculations [9,10,14] for ionization of the $X\,^1\Sigma_g^+(v_i = 0)$ state of H_2.

The MCCC method has recently been applied to scattering on the $v_i = 0$ vibrational level of the $B\,^1\Sigma_u^+$, $c\,^3\Pi_u$, $a\,^3\Sigma_g^+$, $EF\,^1\Sigma_g^+$, and $C\,^1\Pi_u$, states of H_2, including ionization [15]. Agreement with the Gryzinski calculations of Wünderlich [13] was good for the $B\,^1\Sigma_u^+$, $c\,^3\Pi_u$, and $C\,^1\Pi_u$ states, but for the $EF\,^1\Sigma_g^+$ and $a\,^3\Sigma_g^+$ states there is a difference of up to 20% at the cross-section maximum. Calculations by Joshipura et al. [16] using their 'complex scattering potential—ionization contribution' method for ionization of the metastable $c\,^3\Pi_u$ state were also in good agreement with the MCCC and Gryzinski calculations. Aside from MCCC, no other fully quantum-mechanical calculations have been performed for ionization of electronically-excited states.

The total ionization cross section has three main contributions:

(1) non-dissociative ionization with the residual H_2^+ ion being formed in a bound vibrational level of the ground electronic state ($X\,^2\Sigma_g^+$),

(2) dissociative ionization with the ion being formed in the vibrational continuum of the $X\,^2\Sigma_g^+$ state, and

(3) dissociative ionization via the first excited electronic state ($A\,^2\Sigma_u^+$).

The $A\,^2\Sigma_u^+$ state has a repulsive potential energy curve, so excitations of this state always lead to dissociation. For a useful illustration of these processes, see Fig. 1 of Ref. [13]. Ionization leading to excitation of higher electronic states in H_2^+ will also lead to dissociation, however the cross sections for these processes are likely to be negligible. The Gryzinski calculations of Wünderlich [13] consider each of the above three processes in detail in order to provide cross sections for total dissociative and non-dissociative ionization. In the MCCC method, however, it is not currently possible to study the ionization-with-excitation

process (producing H_2^+ in an excited electronic state). Therefore we restrict the present work to considering ionization via the $X\,^2\Sigma_g^+$ state. As seen in Ref. [13] the cross section for this process is generally orders of magnitude larger than for the ionization-with-excitation process.

2. Computational details

The AN MCCC method has been extensively detailed previously [3,15], and the methods used to obtain the ionization cross sections in this work are identical to what is outlined in Ref. [15]. The computational models applied to ionization of the ground state and excited electronic states differ due to the different rates of convergence and the more diffuse nature of some of the excited electronic-state potential-energy curves. Here we provide a brief discussion of the calculations, and refer the interested reader to Ref. [15] for further details of the MCCC method and the extraction of ionization cross sections in the AN approximation. Atomic units are used throughout this paper, unless specified otherwise.

2.1. Ionization of the $X\,^1\Sigma_g^+$ state

The previous papers in this series [4–6], which studied electronically-bound excitations from the $X\,^1\Sigma_g^+$ state, utilized a scattering model with 210 target states in the close-coupling expansion. However, this model does not yield a converged ionization cross section for the $X\,^1\Sigma_g^+$ state at all energies. In the present work we use the 210-state model in the 0–60 eV energy range, where it is sufficiently converged, and a larger 300-state model for higher energies up to 1000 eV. The target states in this model are generated using a Laguerre basis with $N = 12 - \ell$, for ℓ up to 7, and exponential falloffs $\alpha = 0.8$. An accurate H_2^+ ground-state molecular orbital then replaces the 1*s* Laguerre function. The 2*s*, 3*s*, 2*p*, 3*p*, 3*d*, 4*d*, 5*d* and 4*f* orbitals are replaced by Laguerre functions with exponential falloffs

$$\alpha_l = \begin{cases} 1, & l = 0 \\ 1.33, & l \geq 1. \end{cases} \tag{1}$$

See Ref. [15] for definitions of these parameters and details of the structure calculations. This basis produces 977 (pseudo)states, and in the close-coupling calculations we keep the 300 target states with excitation energies below 62 eV (from the ground state at the mean internuclear separation). To account for the small amount of flux into the higher-energy continuum pseudostates, we apply an energy-dependent scaling procedure to ensure at high energies the ionization cross section converges to the analytical Born cross section calculated using the full set of target states.

2.2. Ionization of excited electronic states

For scattering on the $n = 2$ electronic states, we found previously [15] that the 210-state model is sufficient to yield converged cross sections for all processes, including ionization. For some electronic states, such as the $B\,^1\Sigma_u^+$ state, the highest vibrational wave functions can span very large internuclear separations, as large as $R = 50$. We have found that the structure model outlined in Ref. [15], with minor modifications, can be used to generate target wave functions with acceptable accuracy up to $R = 10$. Further discussion of the structure model used here will be given in a following paper on vibrationally-resolved transitions between excited states. For internuclear separations larger than $R = 10$ it is not possible to generate accurate target states without requiring a much larger basis that would make subsequent scattering calculations unfeasible. Since the majority of the vibrational levels in the excited electronic states are contained within $R \leq 10$, we have chosen to limit the vibrational levels to those for which we can guarantee an acceptable accuracy. The number of vibrational levels we include for each state are summarized in Table A. Since the highest vibrational levels are much less likely to be populated in a plasma, we believe this is an acceptable compromise.

Table A
Number of vibrational levels in each electronic state considered in the present work. Entries are presented as v_{max}/v_{tot}, where v_{max} is the number of levels considered here, and v_{tot} is the total number of levels supported by the state.

State	Molecule					
	H_2	HD	HT	D_2	DT	T_2
$X\,^1\Sigma_g^+$	15/15	17/18	18/19	21/22	21/24	23/26
$B\,^1\Sigma_u^+$	28/40	32/46	34/49	39/57	43/62	48/69
$EF\,^1\Sigma_g^+$	25/33	29/39	30/41	35/47	38/52	43/58
$C\,^1\Pi_u$	14/14	16/16	17/17	19/19	21/21	24/24
$a\,^3\Sigma_g^+$	16/22	18/25	19/27	22/31	24/34	27/38
$c\,^3\Pi_u$	17/22	20/26	21/27	25/31	27/34	30/38

3. Cross sections and isotopic effects

Cross sections for ionization of the states listed in Table A have been calculated from threshold up to 1000 eV. In Fig. 1 we compare the $v_i = 0$ cross sections for the different isotopologues and find that there are no noticeable isotopic effects. In Fig. 2 we make a similar comparison but as a function of the initial vibrational level energy at a fixed incident energy near the cross-section maximum (80 eV for the $X\,^1\Sigma_g^+$ state and 16 eV for the $n = 2$ states). Although each isotopologue has a different spectrum of vibrational levels, the cross sections as a function of vibrational-level energy show very little isotope effect. The interesting structure in the $EF\,^1\Sigma_g^+$ cross section is due to the two distinct series in the lower vibrational levels corresponding to the two minima in the $EF\,^1\Sigma_g^+$ potential-energy curve.

In Fig. 3, we compare the $v_i = 0$ ionization cross sections for H_2 with the previous measurements [17–20] and calculations [9,10,16] available in the literature. For the $X\,^1\Sigma_g^+$ state, there is good agreement between all available data. For the excited states, there is surprisingly good agreement between the MCCC cross section and the more approximate Gryzinski and CSP-ic calculations, though for the $EF\,^1\Sigma_g^+$ and $a\,^3\Sigma_g^+$ states there is still a discrepancy of up to 20% at the cross-section peak. More detailed comparisons with the Gryzinski calculations for excited vibrational levels in all six isotopologues are given in Graphs 1–6. As in Fig. 3, there are many cases where the agreement between the two calculations is unexpectedly good, but others where there are substantial discrepancies. There does not appear to be any particular pattern determining which cross sections show good agreement and which do not.

4. Analytic fits

In addition to numerical cross sections, we also provide analytic fits for each transition, employing the following analytic fit function:

$$\sigma(x) = \frac{1}{x}\left[a_0 \ln(x) + \sum_{i=1}^{5} a_i \left(1 - \frac{1}{x}\right)^i\right] \exp\left(-\frac{1}{x^{a_6}}\right) \tag{2}$$

Here, $x = E_{in}/E_0$, where E_0 is the threshold energy. The fitting parameters are also provided in text files as outlined in Section 6. For scattering on excited vibrational levels, it is common for the cross section to be negligible (e.g. less than $10^{-5}\ a_0^2$) for several eV above threshold before suddenly rising. Since these cross sections

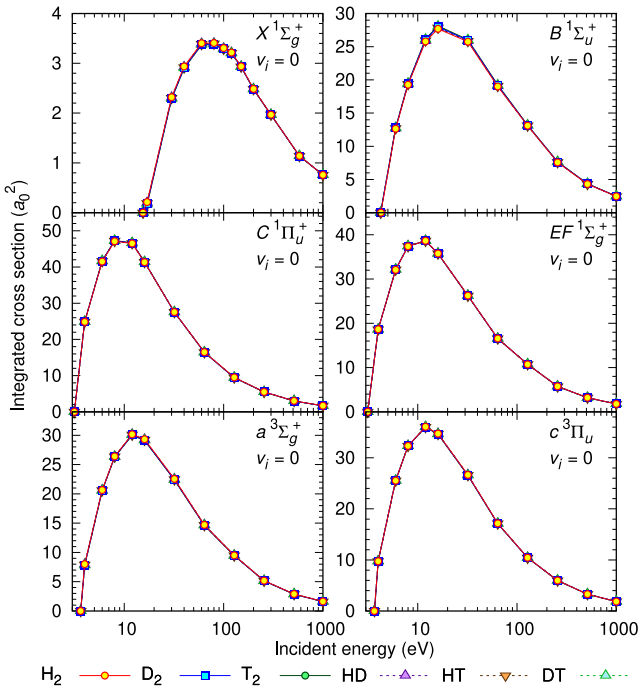

Fig. 1. Total ionization cross sections for H_2, D_2, T_2, HD, HT, and DT from the $v_i = 0$ vibrational level of the $X\,^1\Sigma_g^+$, $B\,^1\Sigma_u^+$, $C\,^1\Pi_u$, $EF\,^1\Sigma_g^+$, $c\,^3\Pi_u$ and $a\,^3\Sigma_g^+$ electronic levels.

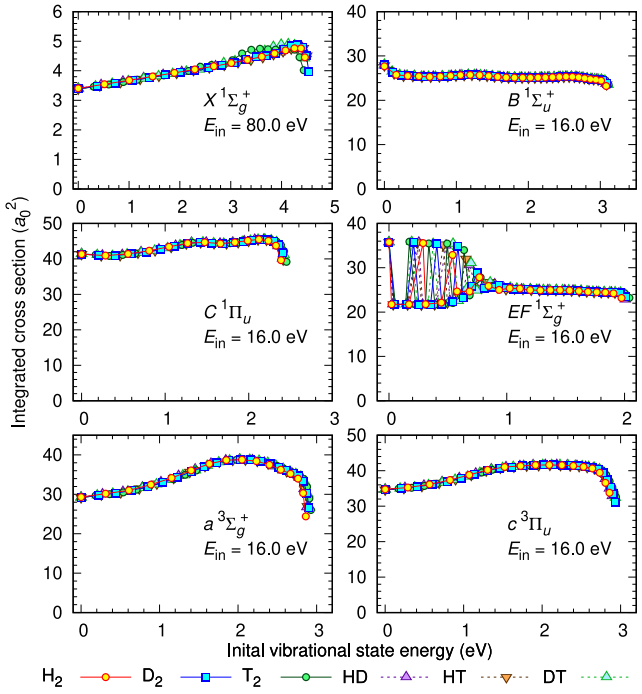

Fig. 2. Total ionization cross sections for H_2, D_2, T_2, HD, HT, and DT as a function of initial vibrational state energy. The results are presented relative to the energy of the $v_i = 0$ vibrational level for each respective electronic state.

represent a sum over the final vibrational levels in the H_2^+ ion, this effect can be explained by the small Franck–Condon (FC) factor between high v_i in H_2 and low v_f in H_2^+. Rather than defining the threshold to be the excitation energy of the $v_f = 0$ level in H_2^+, for the purposes of performing analytical fits it is more convenient to define it as the energy where the cross section

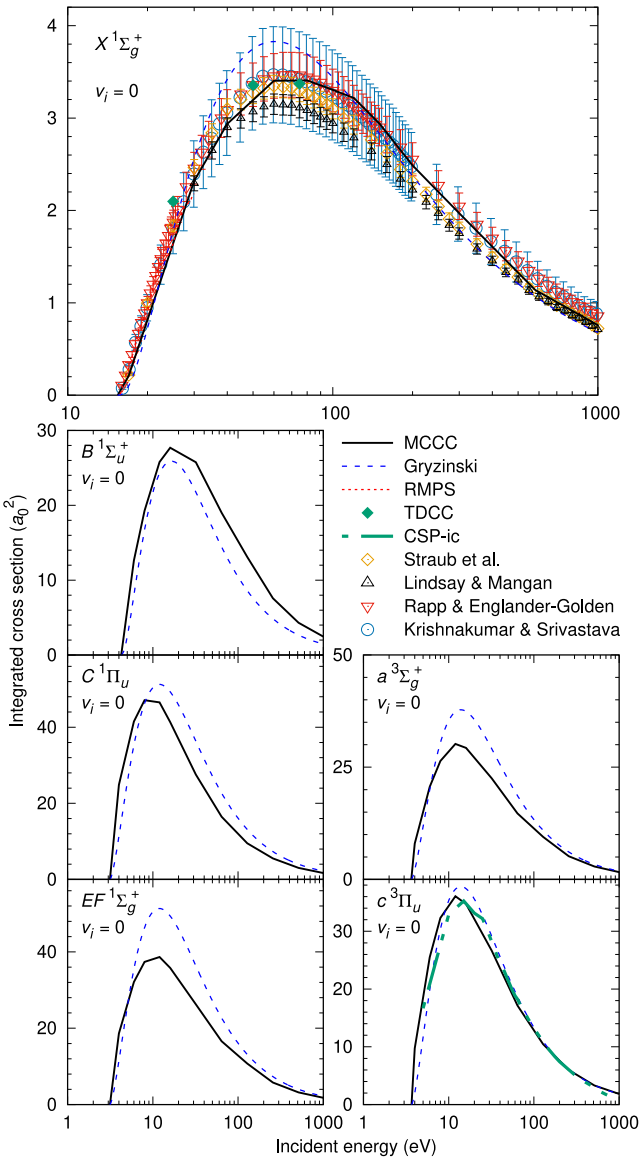

Fig. 3. Ionization cross section for the $v_i = 0$ level of the $X\,^1\Sigma_g^+$, $B\,^1\Sigma_u^+$, $C\,^1\Pi_u$, $EF\,^1\Sigma_g^+$, $a\,^3\Sigma_g^+$ and $c\,^3\Pi_u$ states of H_2. For each state we compare with the Gryzinski calculations of Wünderlich [13]. For the $X\,^1\Sigma_g^+$ state, we also compare with the measurements of Straub et al. [17],Rapp and Englander-Golden [18],Krishnakumar and Srivastava [19] and Lindsay and Mangan [20], the RMPS calculations of Gorfinkiel and Tennyson [9], and the TDCC calculations of Pindzola et al. [10]. For the $c\,^3\Pi_u$ state we compare with the CSP-ic calculations of Joshipura et al. [16]. See the introduction for acronym definitions.

begins to rise substantially. We have found that the excitation energy of the lowest vibrational level of H_2 for which the FC factor is greater than 0.01 (1% of the sum over all v_f) is a suitable choice of threshold for these purposes.

5. Uncertainties

In Ref. [4] we estimated the uncertainties in the numerical cross sections for vibrationally-resolved electronic excitation to be 10%, while for the fitted cross sections we estimated an uncertainty of 12%. In the present work, the various considerations of target structure accuracy, rates of convergence, and accuracy of the fits are much the same, so we provide the same uncertainty estimate of 10% (12%) in the calculated (fitted) cross sections.

Note that the vibrational levels we have considered in this work were chosen according to the requirement that they span internuclear separations $R \leq 10$ where this uncertainty estimate is valid.

6. Accessing the data

The numerical cross sections are provided in supplementary data files named in the format

```
MCCC-el-H2-TICS.[i]_vi=[vi].txt
```

where `TICS` stands for total ionization cross section, `[i]` is the initial electronic state, and `[vi]` is the initial vibrational level. See Appendix 1 of Ref. [4] for details on converting the diatomic state labels to alphanumeric strings. Files containing the fitting parameters are named in the format

```
MCCC-el-H2-TICS.[i]_fit.txt
```

and contain parameters for all vibrational levels of the initial electronic state `[i]`. The cross-section and fitting-parameter files can also be downloaded from the MCCC database website at mccc-db.org. This repository will be continuously updated as new results are produced and is the best location to access the entire set of MCCC cross sections.

7. Conclusions

We have presented vibrationally resolved ionization cross sections for electron scattering on excited vibrational levels in the $X\,^1\Sigma_g^+$, $B\,^1\Sigma_u^+$, $C\,^1\Pi_u$, $EF\,^1\Sigma_g^+$, $a\,^3\Sigma_g^+$, and $c\,^3\Pi_u$ electronic states of H_2, D_2, T_2, HD, HT, and DT. Analytic fits have been provided for all cross sections, and we have estimated an uncertainty of 10% in the numerical data and 12% in the fitted data. The present calculations represent the first comprehensive study of vibrationally-resolved ionization of H_2 using a fully quantum-mechanical method, and we expect the results will be of use in plasma-modeling applications.

Declaration of competing interest

The authors declare that they have no known competing financial interests or personal relationships that could have appeared to influence the work reported in this paper.

Data availability

The MCCC cross sections are available in the supplementary material, and the MCCC database at https://mccc-db.org.

Acknowledgments

We are grateful to Dirk Wünderlich for useful discussions regarding plasma-modeling applications which provided the motivation for the present work. This research was supported by the Australian Government through the Australian Research Council *Discovery Projects* funding scheme (project DP190101195), and by the United States Air Force Office of Scientific Research. The authors acknowledge the Texas Advanced Computing Center (TACC) at The University of Texas at Austin for providing HPC resources that have contributed to the research results reported within this paper. We also acknowledge the support of the Australasian Leadership Computing Grants scheme, with computational resources provided by NCI Australia, an NCRIS enabled capability supported by the Australian Government. Additional HPC resources were provided by the Pawsey Supercomputing Research Centre with funding from the Australian Government and the Government of Western Australia. M.C.Z would like to specifically acknowledge the support of the Los Alamos National Laboratory (LANL), USA Laboratory Directed Research and Development program project number 20200356ER. LANL is operated by Triad National Security, LLC, for the National Nuclear Security Administration of the U.S. Department of Energy under Contract No. 89233218NCA000001.

Appendix A. Supplementary data

Supplementary material related to this article can be found online at https://doi.org/10.1016/j.adt.2023.101573.

References

[1] J.-S. Yoon, M.-Y. Song, D.-C. Kwon, H. Choi, C.-G. Kim, V. Kumar, Phys. Rep. (2014) 199.
[2] D. Wünderlich, L.H. Scarlett, S. Briefi, U. Fantz, M.C. Zammit, D.V. Fursa, I. Bray, J. Phys. D. Appl. Phys. (2021) 115201.
[3] M.C. Zammit, D.V. Fursa, J.S. Savage, I. Bray, J. Phys. B At. Mol. Opt. Phys. (2017a) 123001.
[4] L.H. Scarlett, D.V. Fursa, M.C. Zammit, I. Bray, Yu. Ralchenko, K.D. Davie, At. Data Nucl. Data Tables (2021a) 101361.
[5] L.H. Scarlett, D.V. Fursa, M.C. Zammit, I. Bray, Yu. Ralchenko, At. Data Nucl. Data Tables (2021b) 101403.
[6] L.H. Scarlett, D.K. Boyle, M.C. Zammit, Yu. Ralchenko, I. Bray, D.V. Fursa, At. Data Nucl. Data Tables (2022) 101534.
[7] J.-S. Yoon, M.-Y. Song, J.-M. Han, S.H. Hwang, W.-S. Chang, B. Lee, Y. Itikawa, J. Phys. Chem. Ref. Data (2008) 913.
[8] J.-S. Yoon, Y.-W. Kim, D.-C. Kwon, M.-Y. Song, W.-S. Chang, C.-G. Kim, V. Kumar, B. Lee, Rep. Progr. Phys. (2010) 116401.
[9] J.D. Gorfinkiel, J. Tennyson, J. Phys. B At. Mol. Opt. Phys. (2005) 1607.
[10] M.S. Pindzola, F. Robicheaux, S.D. Loch, J.P. Colgan, Phys. Rev. A (2006) 052706.
[11] X. Liu, D.E. Shemansky, Astrophys. J. (2004) 1132.
[12] R. Celiberto, R. Jenev, A. Laricchiuta, M. Capitelli, J. Wadehra, D. Atems, At. Data Nucl. Data Tables (2001) 161.
[13] D. Wünderlich, At. Data Nucl. Data Tables (2021) 101424.
[14] M.C. Zammit, J.S. Savage, D.V. Fursa, I. Bray, Phys. Rev. A (2017b) 22708.
[15] L.H. Scarlett, J.S. Savage, D.V. Fursa, I. Bray, M.C. Zammit, B.I. Schneider, Phys. Rev. A (2021c) 32802.
[16] K.N. Joshipura, H.N. Kothari, F.A. Shelat, P. Bhowmik, N.J. Mason, J. Phys. B At. Mol. Opt. Phys. (2010) 135207.
[17] H.C. Straub, P. Renault, B.G. Lindsay, K.A. Smith, R.F. Stebbings, Phys. Rev. A (1996) 2146.
[18] D. Rapp, P. Englander-Golden, J. Chem. Phys. (1965) 1464.
[19] E. Krishnakumar, S.K. Srivastava, J. Phys. B At. Mol. Opt. Phys. (1994).
[20] B.G. Lindsay, M.A. Mangan, in Springer-Verlag Berlin Heidelberg, 2003, chap. 5.1.

Explanation of Graphs

Graph 1 **Ionization cross sections for electron collisions with H_2.**

Each row represents a different initial electronic state as labeled in the first panel of the row. Each column represents a different initial vibrational level (v_i) as labeled in each panel. For each state, four values of v_i are chosen for presentation, with the first being $v_i = 0$ and the last being the highest vibrational level we have performed calculations for (see Table A). Comparison is made between the present MCCC calculations and the Gryzinski calculations of Wünderlich [13].

Graph 2 **Ionization cross sections for electron collisions with D_2.**

Graph 3 **Ionization cross sections for electron collisions with T_2.**

Graph 4 **Ionization cross sections for electron collisions with HD.**

Graph 5 **Ionization cross sections for electron collisions with HT.**

Graph 6 **Ionization cross sections for electron collisions with DT.**

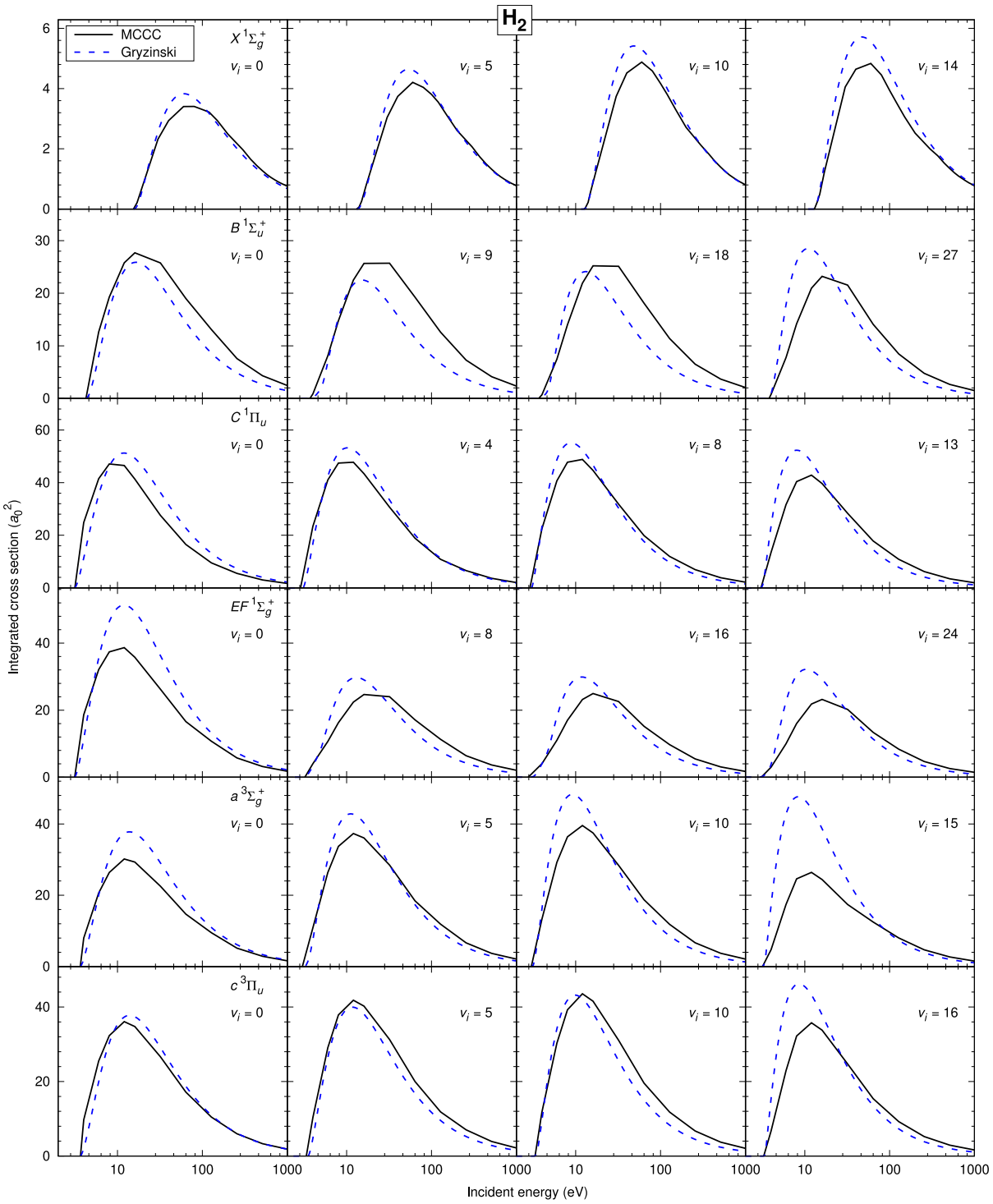

Graph 1. Ionization cross sections for electron collisions with H_2.

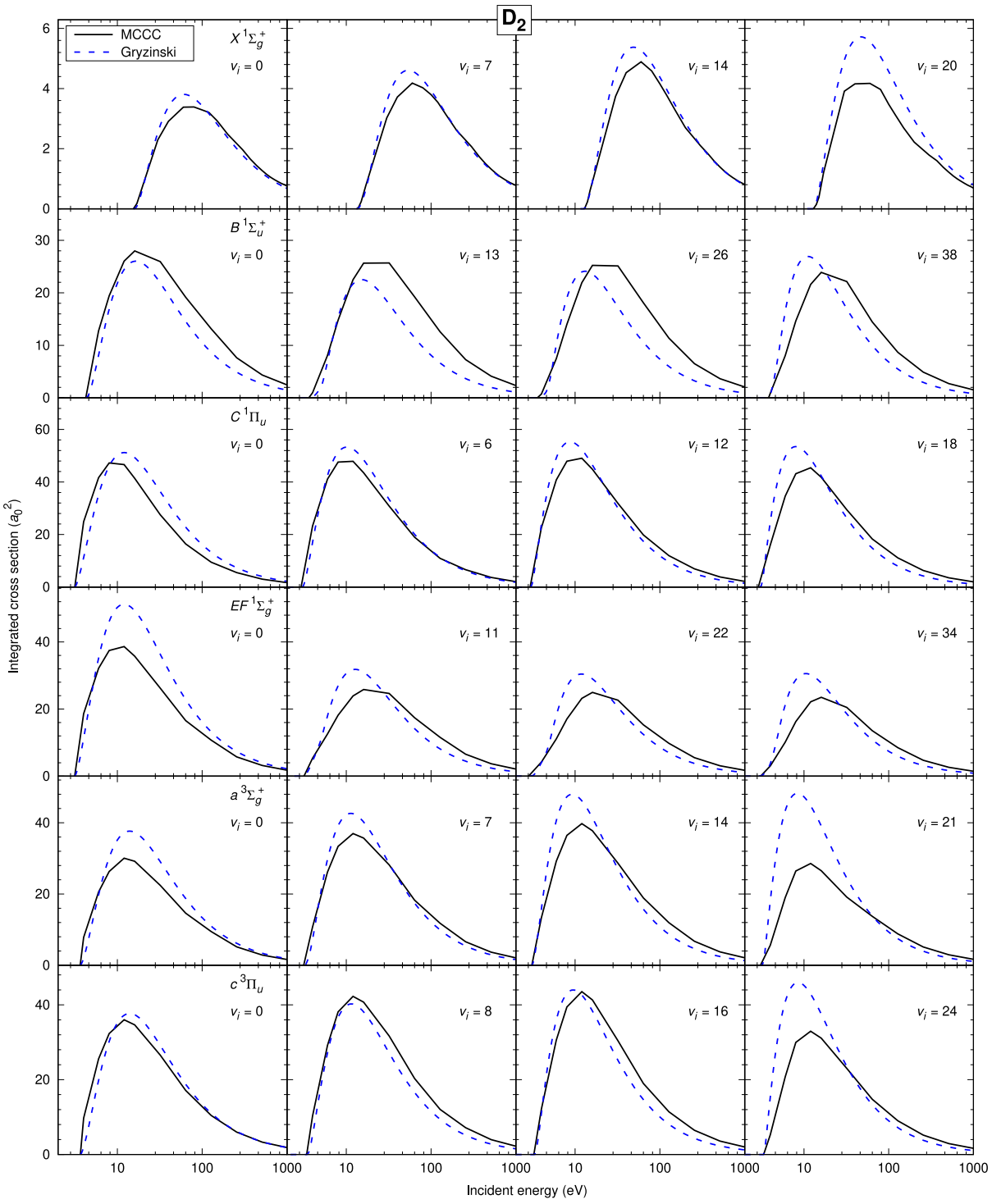

Graph 2. Ionization cross sections for electron collisions with D_2.

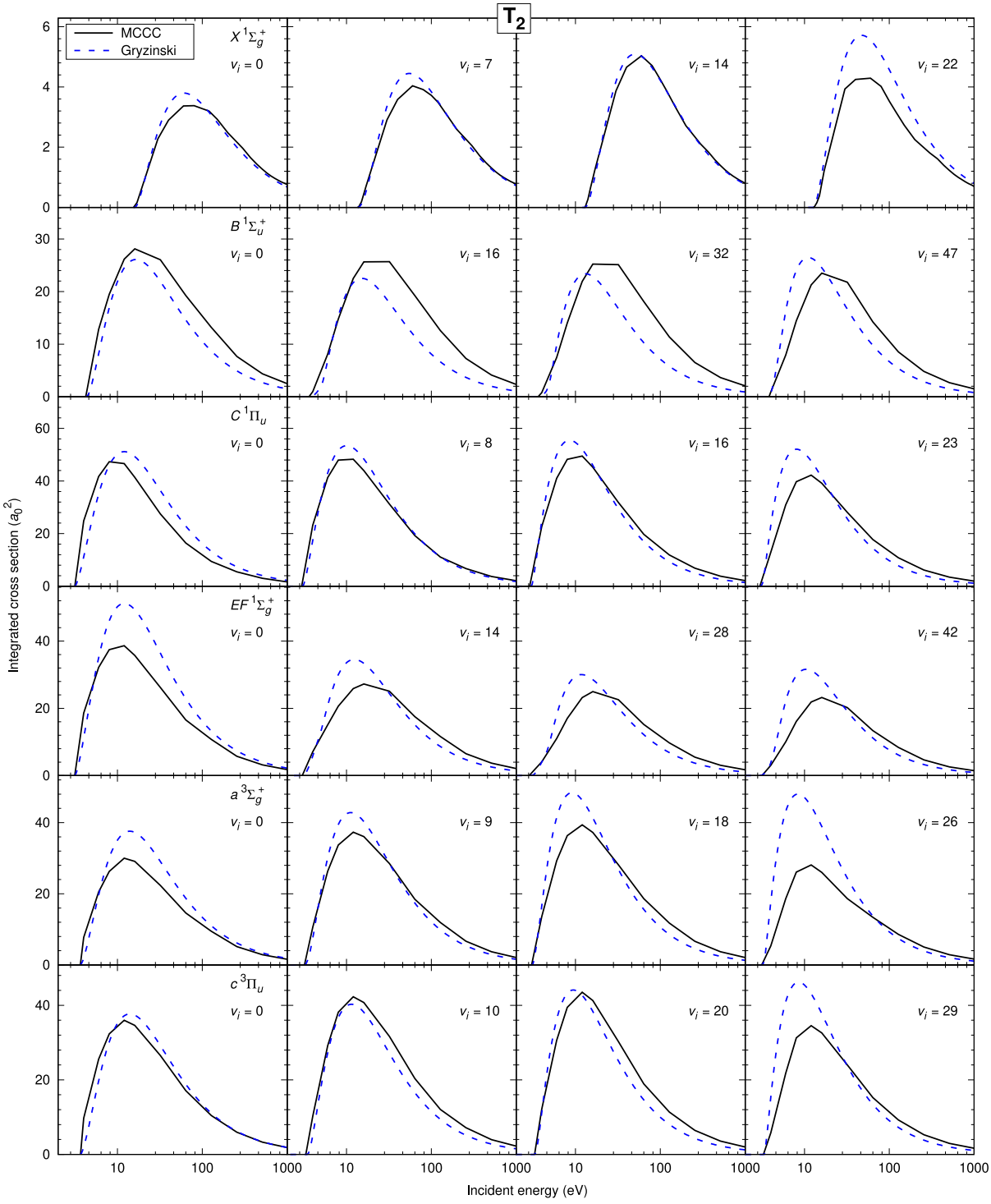

Graph 3. Ionization cross sections for electron collisions with T_2.

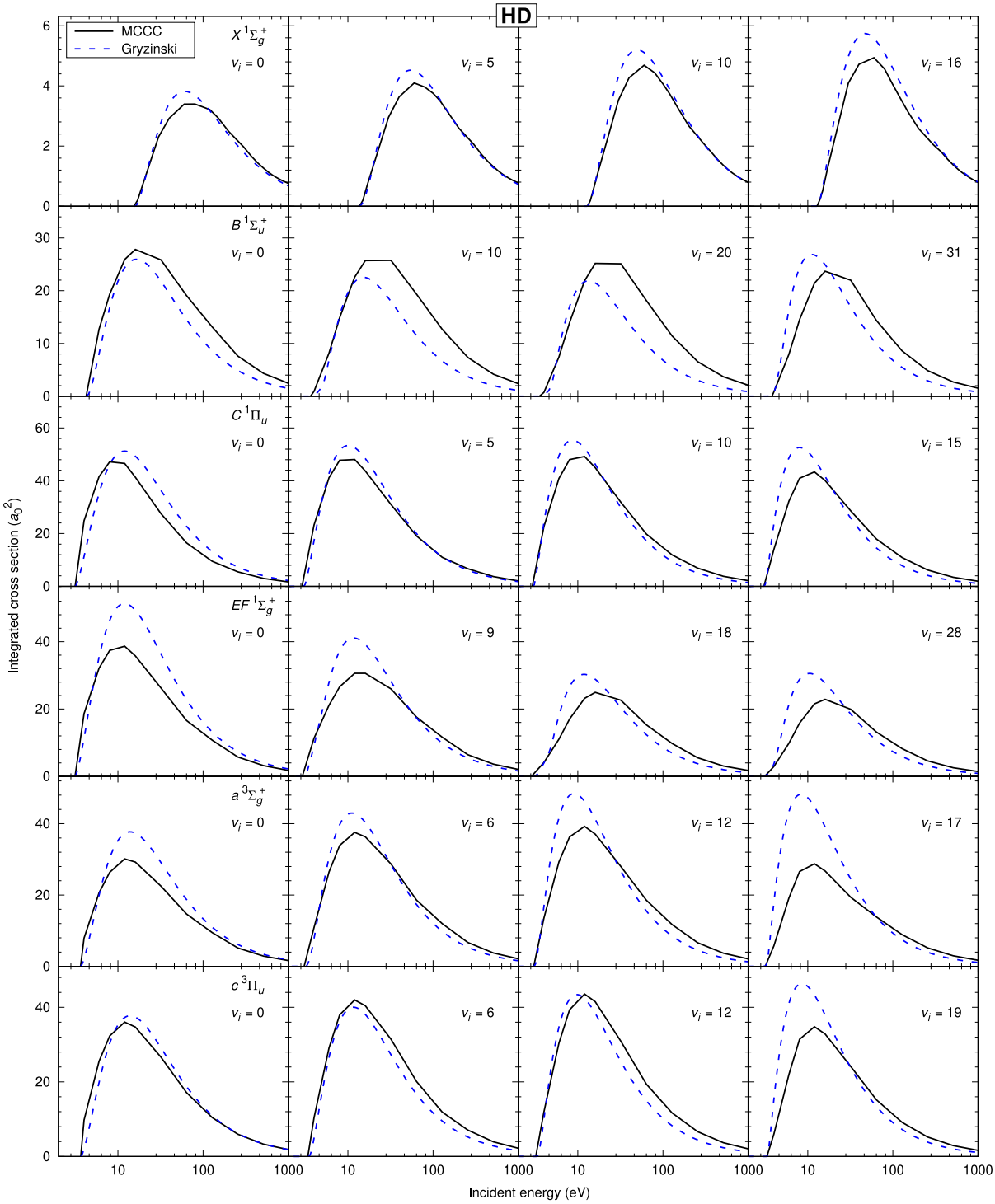

Graph 4. Ionization cross sections for electron collisions with HD.

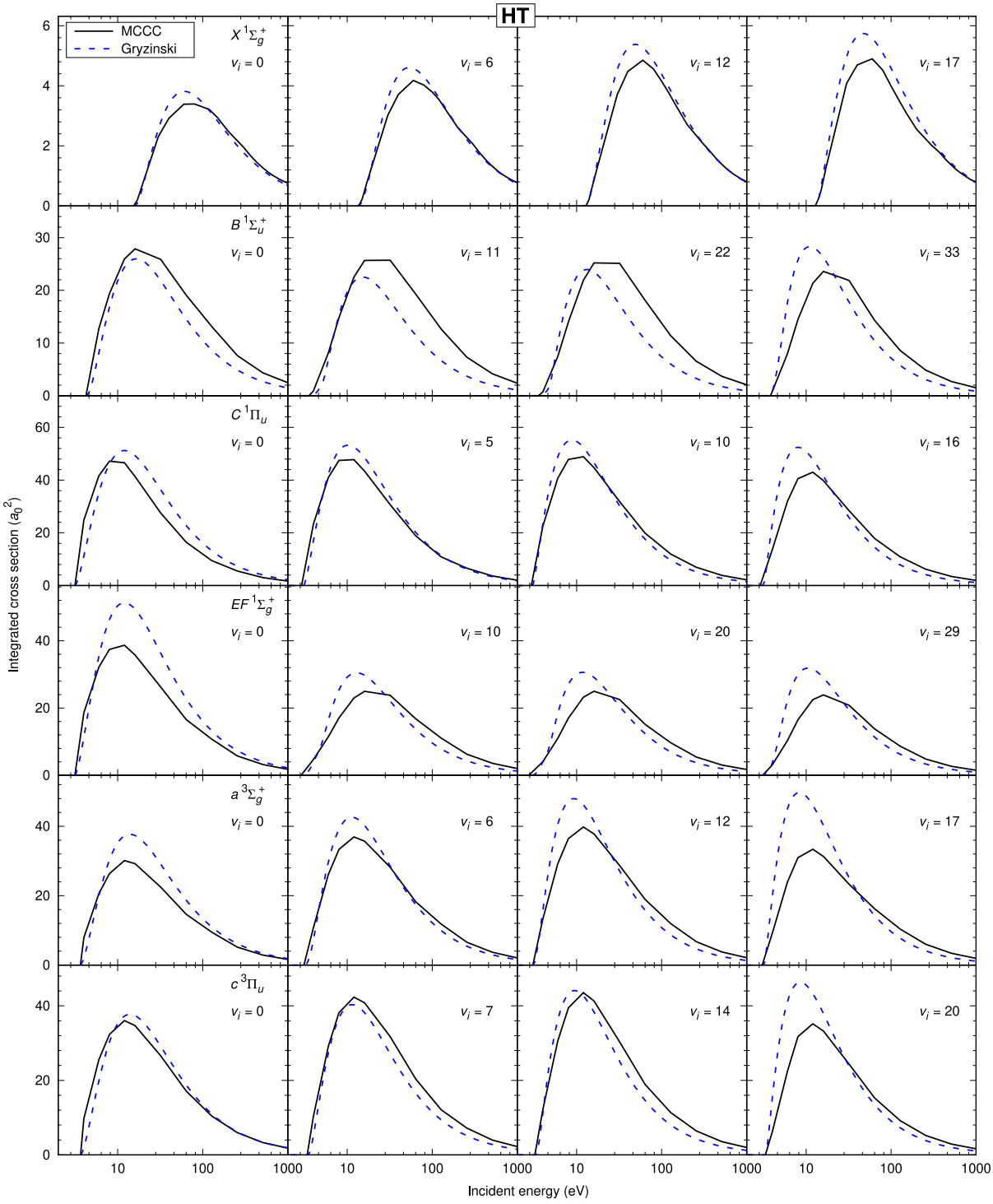

Graph 5. Ionization cross sections for electron collisions with HT.

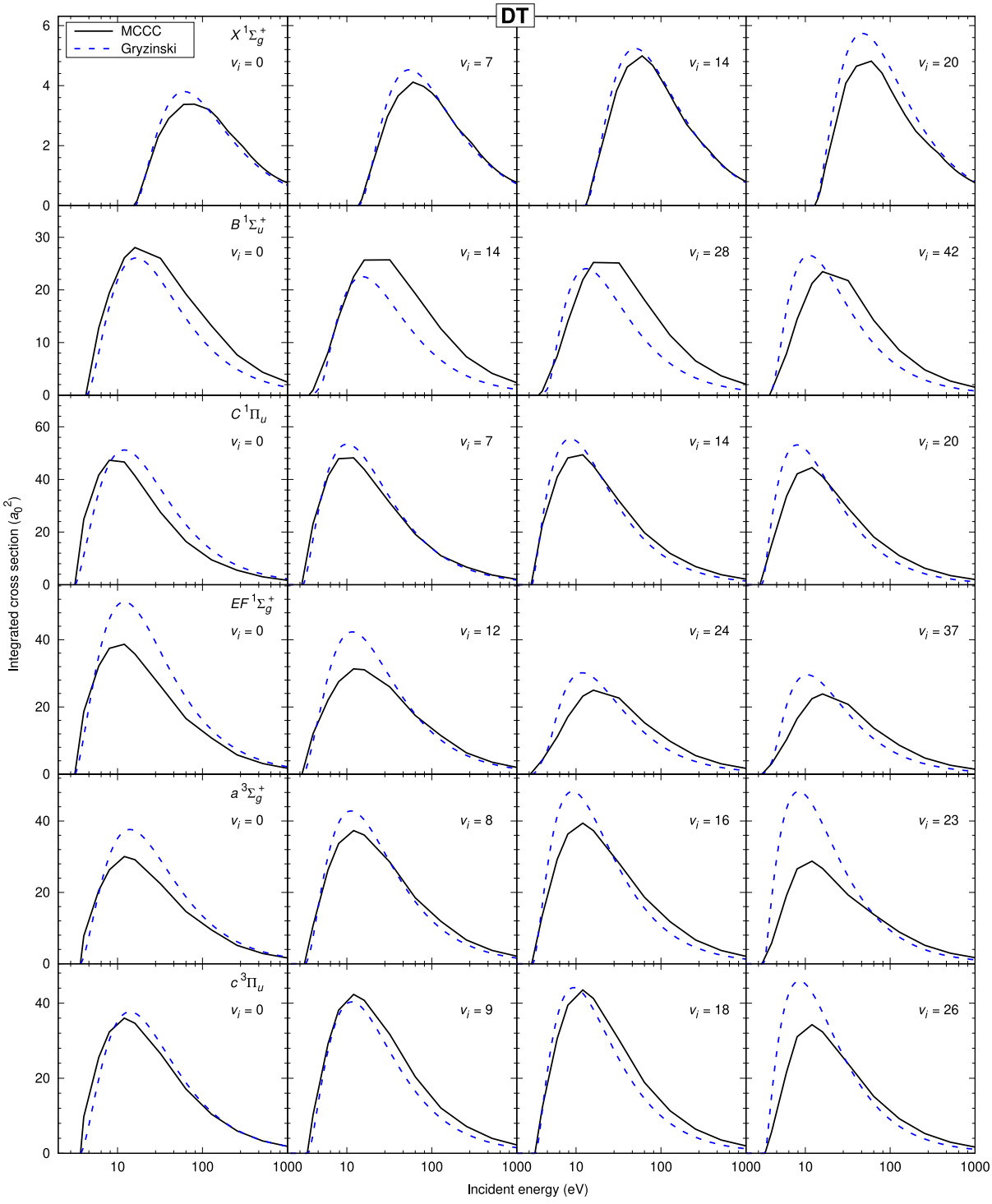

Graph 6. Ionization cross sections for electron collisions with DT.